Modelling and Characterization of Partial Discharge Activity versus Applied Voltage, Test Frequency and Temperature

Erling Ildstad
Department of Electric Power Engineering
Norwegian University of Technology and Science (NTNU)
Trondheim, Norway
erling.ildstad@ntnu.no

Torstein Grav Aakre
Department of Electric Power Technology
SINTEF Energy Research
Trondheim, Norway
https://orcid.org/0000-0002-9206-185X

***Abstract*— Measurements of partial discharges (PDs) are commonly used as diagnostic indicators for assessing the quality of high voltage equipment. In many cases, such PD measurements are of practical reasons either performed at on-line service stresses or at very low frequency (VLF) off-line tests. This paper aims at providing some insight into how PD parameters determined during VLF off-line testing relate to PD activity occurring at 50 Hz service conditions. The theoretical analysis is based on the classical abc-model applied on glass fibre reinforced epoxy-mica samples including void enclosure with diameter of 10 mm. The PD-activity was examined at test frequencies from 0.1 Hz to 300 Hz, and the temperature was varied in the range from 20 °C to 90 °C. The PD inception voltage was found to be frequency independent, while the maximum apparent charge magnitudes were found to increase with increasing voltage frequency. A high number of low magnitude PDs were observed at low frequencies, which strongly indicate that just a fraction of the void surface is involved in each discharge. It is shown that the total accumulated apparent charge per voltage period is a rather frequency independent parameter, strongly correlated to the average dissipated partial discharge energy.**

Keywords*— Diagnostic testing, partial discharges, cavities, variable voltage frequency

I. Introduction

Results from measurements of partial discharge (PD) activity are commonly used as diagnostic indicators for assessing the quality and condition of many types of high voltage power equipment. Such PD measurements are either performed on-line at service stress or off-line at variable voltage levels and frequencies in the range from 0.1 Hz to 50 Hz. Very low frequency (VLF) off-line testing is particularly beneficial when performing diagnostic testing of test objects with large capacitance to ground, for example cables and generators [1], allowing a lightweight voltage source to be used to energize the test object. There have been conducted some studies to investigate the voltage frequency dependence in the range of 0.01 Hz to 100 Hz. Both large cylindrical voids and spherical voids have been studied [2][3], but the frequency behaviour varies. A resent review [4] summarizes the same conclusions with more relevant references included. It is therefore necessary to improve knowledge and experience regarding how results from VLF measurements relate to what PD activity is expected at power frequencies. During on-site measurements the temperature of the insulation may vary. The temperature variation is for example caused by different current load history and cooling conditions. This makes it difficult to evaluate results from PD-diagnostic tests, based upon trend analysis as well as comparison of power equipment with similar types of insulation systems.

This paper addresses these basic challenges, aiming mainly at providing some insight into the correlation between PD parameters determined during VLF and 50 Hz voltage testing. The classical equivalent abc-model is used to express theoretical relations between void discharges and measurable quantities. Laboratory experiments were performed using small plaques of glass fibre reinforced epoxy/mica insulation with cylindrical void enclosures.

II. Theory

By the so-called abc model, shown in Fig.1b, each insulation section of the test object is considered as a capacitance; where the void is represented by a capacitance c in series with an insulation section of capacitance b, whereas the remaining surrounding void-free insulation is represented by the parallel capacitance a. It is common to slightly modify the equivalent circuit by adding resistances in parallel to the capacitances, as shown in Fig.1c, facilitating study of possible low frequency effects. The main benefit of these simplified electrical equivalents is, however, that standard circuit analysis can be used to approximately characterize and relate the rapid physical discharge processes occurring within voids to external measurable quantities as; PD inception- and extinction voltage (PDIV and PDEV), apparent charge magnitude, PD repetition rate and dissipated energy.

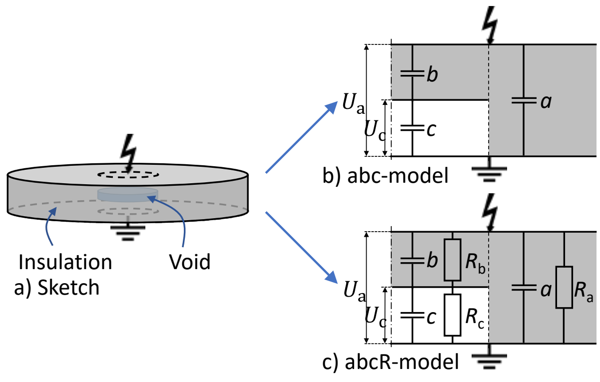

Fig. 1: Representation of a) a sample with a cylindrical void. b) The abc-equivalent model of the test object and c) the resistance modified abc-model.

A. PDIV

Upon increasing the applied test voltage magnitude, PDs occur at the location where the local electric stress exceeds the critical breakdown strength. Usually voids within a solid insulation system are such critical weak locations. The

This work is funded by the project "Hydrogenerator Stator Winding Insulation Assessment". The project is supported by The Research Council of Norway (Project No. 255099/E20), and industrial partners.

978-1-6654-8491-6/22/$31.00 ©2022 IEEE

This is the accepted version of a paper presented at 2022 IEEE 4th International Conference on Dielectrics - ICD
http://dx.doi.org/10.1109/ICD53806.2022.9863553

applied voltage when PD starts is called the partial discharge inception voltage (PDIV).

The equivalent abc-model can be used to express a relation between the applied voltage U_a and the resulting voltage across the void U_c. Considering the general abc-model, including insulation resistances, the resulting voltage across the void becomes expressed by:

$$U_\mathrm{c} = \frac{1}{1 + \frac{1/R_c + \omega \cdot c}{1/R_b + \omega \cdot b}} \cdot U_\mathrm{a} \tag{1}$$

This means that the PDIV is expected to vary with the magnitude and frequency of the applied voltage as well as the ratio between the conductivities and permittivities of the insulation sections involved.

Detailed knowledge of number and exact shape of enclosed voids are, however, rarely known. For simplicity, it is therefore common to consider PD inception occurring at a void breakdown voltage expressed by the empirical Paschen relation [5]:

$$U_\mathrm{cs} = 2.12\sqrt{pd_\mathrm{c}} + 2.44(pd_\mathrm{c})\ [\mathrm{kV_{peak}}] \tag{2}$$

found to be valid for breakdown of air in homogeneous electric field and metallic electrode at gas pressure times void gap distance (pd_c) in the range from 10^{-1} to $5{\cdot}10^{3}$ [bar·mm].

B. The apparent charge magnitude

During the short duration of a discharge, it is practically impossible to measure the instantaneous voltage drop ΔU_c across the void or the magnitude of the exchanged internal charge q_i. Immediately after the PD is extinguished, a transient current flow in the external circuit, compensating for the voltage drop ΔU_a across the test object. The magnitude of this measurable current pulse is then calibrated to represent the so-called apparent charge magnitude q_a:

$$q_\mathrm{a} = \frac{b}{a+b}\left(a + \frac{bc}{b+c}\right)\Delta U_\mathrm{c} \approx b \cdot \Delta U_\mathrm{c} \tag{3}$$

The latter approximation is valid in the cases $a \gg b$ and c. Accordingly, the apparent charge magnitude q_a is expected to increase proportionally with the magnitude of the instantaneous voltage drops across the void, ΔU_c. In addition, the shape and the actual surface area involved in the void discharge strongly affect the magnitude of the observed apparent charge.

C. PD repetition rate per voltage period

Considering an ideal situation, the average expected number of PDs per voltage period is given as:

$$n_0 = \frac{2 \cdot \left(\frac{b}{b+c} U_\mathrm{a} - U_\mathrm{r}\right)}{\Delta U_\mathrm{c}} \tag{4}$$

Assuming low values of remnant voltage U_r compared to that of the applied voltage magnitude U_a and the voltage drop across the void, ΔU_c, by combining Equations (3) and (4) gives that the number of PDs per period can be expressed by:

$$n_0 = 2 \cdot \frac{b}{a+b}\left(a + \frac{bc}{b+c}\right)\frac{b}{b+c} \cdot \frac{U_\mathrm{a}}{q_\mathrm{a}} = A \cdot \frac{U_\mathrm{a}}{q_\mathrm{a}} \tag{5}$$

where A is a capacitive geometric parameter. Thus, above the PDIV the number of PDs is expected to increase linearly with the magnitude of the applied voltage, whereas a higher number of discharges is expected in the case of small magnitude PDs.

D. Dissipated energy and total apparent charge

The energy dissipated in a cavity during a discharge can be considered as the energy delivered from the external voltage source at the instant of PD. The total dissipated energy during a certain time T is then expressed by [6]:

$$\Delta W_\mathrm{T} = \sum_{i=1}^{i=n} q_\mathrm{a}^i \cdot U_\mathrm{a}^i \tag{6}$$

where q_a^i is the apparent charge of the i^{th} discharge, U_a^i the instantaneous voltage applied across the test object at the time of the i^{th} discharge and n is the total number of discharges occurring during the examined interval T.

If the PDs are distributed in a certain range around an average applied voltage $\langle U_i \rangle$, the energy delivered per period can approximately be expressed as:

$$W = \langle U_i \rangle \cdot \sum_{i=1}^{i=n_0} q_\mathrm{a}^i = \langle U_i \rangle \cdot q_\mathrm{a}^T \tag{7}$$

where q_a^T represents the total measured apparent charge per period:

$$q_\mathrm{a}^T = \sum_{i=1}^{i=n_0} q_\mathrm{a}^i = x \cdot n_0 \cdot q_\mathrm{a}^0 \tag{8}$$

where $n_0 \cdot q_\mathrm{a}^0$ is the expected total apparent charge if the entire void is discharged in accordance with the abc-model. The ratio factor x is included to consider actual cases where only a fraction x of the void is involved in each discharge.

III. Methodology

To experimentally examine the effects of voltage frequency and temperature, 3 mm thick test objects were made using two 1.5 mm thick pre-shaped and cured layers made of glass fibre reinforced resin-rich epoxy mica tape. These plaques were pre-shaped in a mould and then cured for one hour at 160 °C. In one of the layers, a void was formed by applying a metal disk as a spacer during the casting process. This resulted, as shown in Fig. 2, in a 10 mm wide void enclosure with a gap distance d_c of 0.5 mm. The average values from examination of three equal test objects were presented.

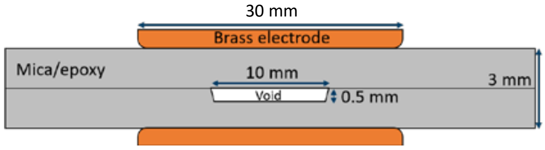

Fig. 2: Dimensions of the glass fibre reinforced mica/epoxy insulated test object with a cylindrical void.

During testing the test objects were clamped between two brass electrodes. To avoid unintended external PD activity the 30 mm wide cylindrical high voltage electrodes were encapsulated in epoxy and in addition silicon grease was

This is the accepted version of a paper presented at 2022 IEEE 4th International Conference on Dielectrics - ICD
http://dx.doi.org/10.1109/ICD53806.2022.9863553

applied between the metal electrodes and the surface of the samples

All measurements were performed using a phase resolved PD acquisition unit MPD 600 in a standard direct PD test setup [7]. As shown in Fig. 3, the test object, with a total capacitance of about 20 pF, was connected in parallel to a coupling capacitor of 100 pF. Sinusoidal test voltages at various magnitudes and frequencies were applied using a high voltage amplifier (TREK 20/20B). Sufficient noise reduction was obtained by installing a low-pass filter, with a cut-off frequency at 5 kHz, between the voltage source and the test object. The temperature was varied by keeping the samples in an oven. A fully automated LabView controlled test procedure was utilized to facilitate equal test conditions at different test voltages and temperatures up to maximum 90 °C.

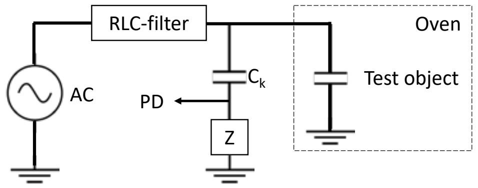

Fig. 3: Schematics of the direct PD test setup used

Prior to PD testing all samples were preconditioned, using a procedure based on the recommendations of [7] and [8]. During an initial 5-minute-long preconditioning period a 50 Hz test voltage was applied at the maximum test magnitude of 10 kV_{rms}. Then, after a 10 s long period of grounding, the PD measurements were performed at selected frequencies, gradually increasing the applied voltage and subsequently decreasing it in steps of 1 kV_{rms} per 10 seconds.

At a certain temperature, the voltage step- and frequency sweep tests were started at 300 Hz and ended at the lowest 0.1 Hz voltage frequency. A total of 12 frequency runs were performed at each temperature allowing a 10 second long 50 Hz preconditioning period between each run.

When varying the temperature in the range of 20 °C to 90 °C a waiting time of one hour was used to reach the new steady state oven temperature, during which period no voltage was applied.

IV. Results and Discussion

A. PDIV

The measured PDIV values presented in Fig. 4, show that PDIV was found to be nearly frequency independent at 60 °C and 90 °C. According to Equation 1, PD inception of the examined sample is expected to occur an applied voltage of 4 kV_{rms}. This is a value in good agreement with the observed values, particularly at the highest temperatures.

If reduced insulation resistances affect the electric field distribution within the test object, the measured PDIV values should according to theory increase at low test frequencies. Such a minor effect was possibly seen for 40 °C. However, at 20 °C the PDIV was found to be higher than the maximum applied 10 kV_{rms} of the power source. This indicate that the increased breakdown strength of the void at the lowest temperatures.

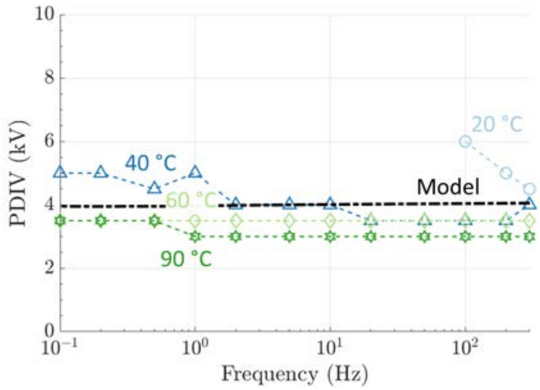

Fig. 4: Measured PDIV (rms) as a function of applied voltage frequency at indicated temperatures. The theoretical curve is based upon the capacitive abc-model.

B. Apparent charge and repetition rate

The measured apparent charge values, presented in Fig. 5 and Fig. 6, indicate several characteristic features:

- The maximum apparent charge magnitudes were found to be close to the theoretically expected values in the case of an entire void discharge; q_{a0}. According to Equation (3), this strongly indicate that only sections of the void are involved in each discharge.
- The repetition rate of the most likely PDs increases fairly linear with the applied voltage magnitude, thus following the expected voltage dependence expressed by Equation (5).
- The additional data presented in Fig. 6 show that the magnitudes of the measured apparent charge vary over a wide range at all test frequencies. An increased number of low magnitude PDs in all examined cases, particularly so at the lowest voltage frequencies, were seen.

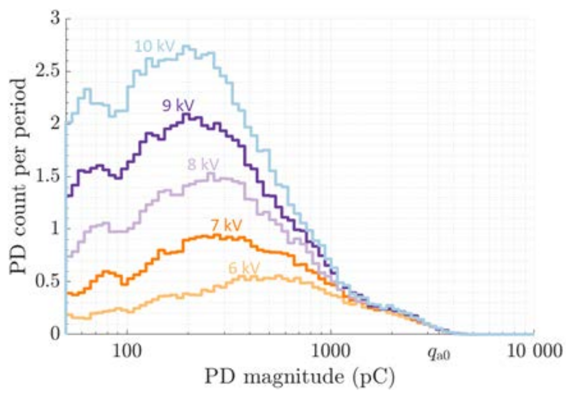

Fig. 5: Measured PD repetition rate per period as a function of PD magnitude for different applied voltages (rms). This typical example has an applied voltage frequency of 50 Hz and temperature of 90 °C. The theoretical value according to Equation (3) is denoted q_{a0} at the x-axis.

This is the accepted version of a paper presented at 2022 IEEE 4th International Conference on Dielectrics - ICD
http://dx.doi.org/10.1109/ICD53806.2022.9863553

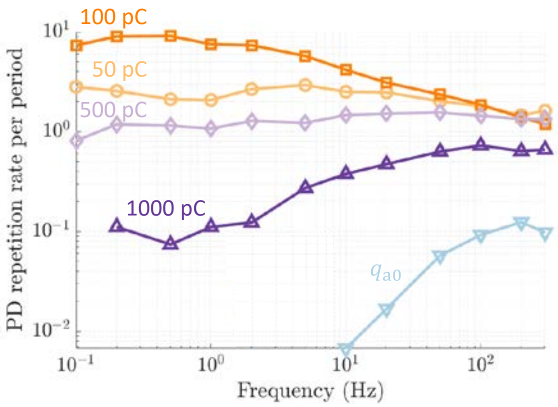

Fig. 6: Measured PD repetition rate versus voltage frequency at10 kV_{rms}, and the indicated apparent charge magnitudes.

Instead of detecting the distribution of all apparent charge magnitudes, it can be argued that the maximum apparent charge, which is observed within a certain test period, is a parameter that more directly correlates to the less frequent discharge of the entire void.

Results presented in Fig. 7 show that the measured maximum apparent charge magnitudes were highly temperature dependent and strongly increase with increasing test temperature at all voltage frequencies. The observed values were not in agreement with the expected theoretical values, particularly so at the highest temperatures and the lowest voltage frequencies. One may speculate that such deviation is caused by several factors, related to both reduced breakdown probability at low temperatures, insufficient measuring time at low voltage frequencies and possible measurement errors in the case of high number of PDs at the highest temperatures.

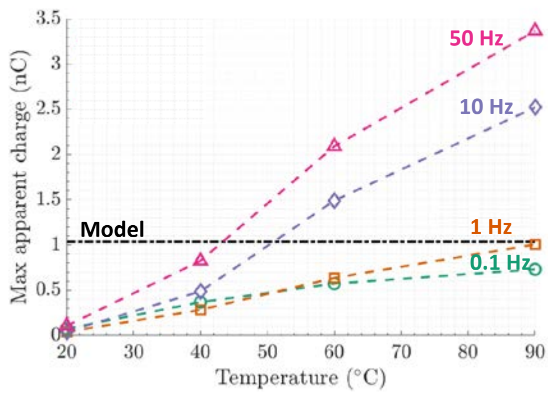

Fig. 7: Measured maximum apparent charge per 10 second period versus temperature at the indicated voltage frequencies at 10 kV_{rms}. The theoretical graph (Model) values are based upon Equation (3) representing discharge of the entire void.

C. Dissipated energy and total apparent charge

The data presented in Fig. 8 show that measured values of total apparent charge strongly increased with increasing temperature but were found to be relatively frequency independent. According to the presented theory, Equation (7), the average dissipated PD energy is expected to be proportional to the total apparent charge. Thus, provided the temperature is known, diagnostic measurements of either total apparent charge or dissipated PD energy at a certain voltage frequency, can be used to predict expected PD activity at another frequency.

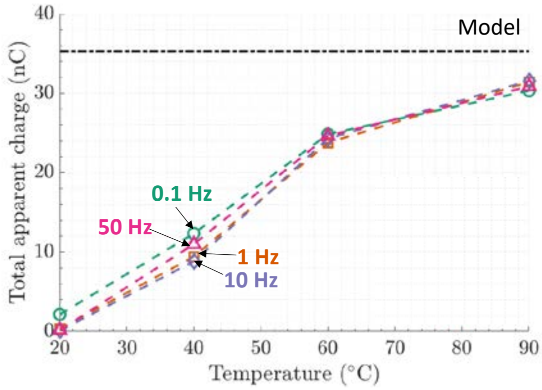

Fig. 8: Measured total apparent charge per period as a function of temperature at the indicated voltage frequencies at10 kV_{rms}. The Model-graph represents a complete discharge of the geometric area $x = 1$ in Equation (8).

V. Conclusions

- Experiments show that both distribution of apparent PD magnitude as well as the maximum values are strongly varying with voltage frequency and temperature. Thus, making these parameters less suitable for interpretation of results obtained during diagnostic low frequency with respect to that at service conditions.
- An alternative approach is to use less frequency dependent parameters, such as the total apparent charge and the dissipated PD energy per period.

References

[1] "IEEE Recommended Practice for Insulation Testing of AC Electric Machinery with High Voltage at Very Low Frequency," IEEE.

[2] C. Forssen and H. Edin, "Partial discharges in a cavity at variable applied frequency part 1: measurements," *IEEE Trans. Dielect. Electr. Insul.*, vol. 15, no. 6, pp. 1601–1609, Dec. 2008

[3] A. Cavallini and G. C. Montanari, "Effect of supply voltage frequency on testing of insulation system," *IEEE Trans. Dielect. Electr. Insul.*, vol. 13, no. 1, pp. 111–121, Feb. 2006

[4] T. Venge and C. Nyamupangedengu, "Influence of Variable Frequency of the Applied Voltage on Cavity Partial Discharge Parameters: A Critical Review," in *2019 Southern African Universities Power Engineering Conference/Robotics and Mechatronics/Pattern Recognition Association of South Africa (SAUPEC/RobMech/PRASA)*, Bloemfontein, South Africa, Jan. 2019, pp. 582–587.

[5] E. Kuffel, W. Zaengl, and J. Kuffel, *High Voltage Engineering Fundamentals, 2nd Edition*. 2000.

[6] R. Bartnikas and R. Morin, "Multi-stress aging of stator bars with electrical, thermal, and mechanical stresses as simultaneous acceleration factors," in *IEEE Transactions on Energy Conversion*, vol. 19, no. 4, pp. 702-714, Dec. 2004

[8] "IEC TS 60034-27:2006, Off-line partial discharge measurements on the stator winding insulation of rotating electrical machines," 2006.

[8] "IEEE Guide for the Measurement of Partial Discharges in AC Electric Machinery,"

This is the accepted version of a paper presented at 2022 IEEE 4th International Conference on Dielectrics - ICD
http://dx.doi.org/10.1109/ICD53806.2022.9863553